JCB Article

p190RhoGAP is cell cycle regulated and affects cytokinesis

Ling Su, Joyce M. Agati, and Sarah J. Parsons

Department of Microbiology and The Cancer Center, University of Virginia Health System, Charlottesville, VA 22908

p190RhoGAP (p190), a Rho family GTPase-activating protein, regulates actin stress fiber dynamics via hydrolysis of Rho-GTP. Recent data suggest that p190 also regulates cell proliferation. To gain insights into the cellular process(es) affected by p190, we altered its levels by conditional or transient overexpression. Overexpression of p190 resulted in a multinucleated phenotype that was dependent on the GTPase-activating protein domain. Confocal immunofluorescence microscopy revealed that both endogenous and exogenous p190 localized to the newly forming and contracting cleavage furrow of dividing cells. However, overexpression of p190 resulted in abnormal positioning of the furrow specification site and unequal daughter cell partitioning, as well as faulty furrow contraction and multinucleation. Furthermore, levels of endogenous p190 protein were transiently decreased in late mitosis via an ubiquitin-mediated degradation process that required the NH_2-terminal GTP-binding region of p190. These results suggest that a cell cycle–regulated reduction in endogenous p190 levels is linked to completion of cytokinesis and generation of viable cell progeny.

Introduction

The process of cytokinesis is a coordinated series of events that occurs in late mitosis. Cytokinesis is initiated by specification of the cleavage plane, followed by: furrow assembly and ingression; midbody formation; and cell separation, which results in the production of two daughter cells, each with an equal complement of chromosomes and membrane (Prokopenko et al., 2000; Glotzer, 2001; Zeitlin and Sullivan, 2001).

Although many works indicate that cleavage plane initiation site selection and cleavage furrow assembly are mediated by the mitotic spindle (Rappaport, 1997; Bonaccorsi et al., 1998), the molecular events that link the mitotic spindle to the newly forming contractile ring are just beginning to emerge (Dechant and Glotzer, 2003; Gonzalez, 2003; Somers and Saint, 2003). Furrow formation involves the assembly of an actin-myosin network, a process that is regulated by the small G protein, Rho. One model, derived from the recent work of multiple investigators, suggests that the initial positioning of the furrow is specified in part by a Rac/Rho GTPase-activating protein (GAP; MgcRacGAP in humans, RacGAP50C in *Drosophila melanogaster*, and Cyk-4 in *Caenorhabditis elegans*), that moves to the spindle midzone by means of binding to a kinesin-like molecular motor (CHO1 in humans, Pavarotti in *Drosophila*, and Zen-4 in *C. elegans*). There, the Rho family GAP interacts with a cortical RhoGEF (ECT2 in humans; and Pebble in *Drosophila*), resulting in the local activation of Rho. The timing of this complex formation is regulated by the destruction of cyclin B and cyclin B3. Together, these events form a scenario in which the molecular motor-Rac–RhoGAP-RhoGEF-Rho complex positions the cleavage specification site by juxtaposing the spindle midzone to cortical actin. The subsequent stage, cleavage furrow formation and contraction, involves assembly of myosin II, actin filaments, septins, and actin-interacting proteins, such as profilin and cofilin, as well as downstream targets of RhoA, including ROCK, citron kinase, LIM kinase, and formin-homology proteins. Thus, Rho can influence cleavage furrow ingression, as well as the specification site selection.

That RhoGTP is critical for these events is supported by the finding that levels of active Rho are increased during cytokinesis, and these elevated levels are required for completion of cytokinesis (Bishop and Hall, 2000; Prokopenko et al., 2000; Glotzer, 2001). To achieve and maintain Rho in its appropriate state of activation during initiation and

L. Su and J.M. Agati have contributed equally to this paper.

The online version of this paper contains supplemental material.

Address correspondence to S.J. Parsons, Dept. of Microbiology and Cancer Center, University of Virginia Health System, P.O. Box 800734, Charlottesville, VA 22908. Tel.: (434) 924-2352. Fax: (434) 982-0689. email: sap@virginia.edu

Key words: Rho; cell cycle; mitosis; ubiquitination; degradation

Abbreviations used in this paper: D-box, destruction box; Dox, doxycycline; GAP, GTPase-activating protein; GBD, GTP-binding domain; MD, middle domain; p190, p190RhoGAP.

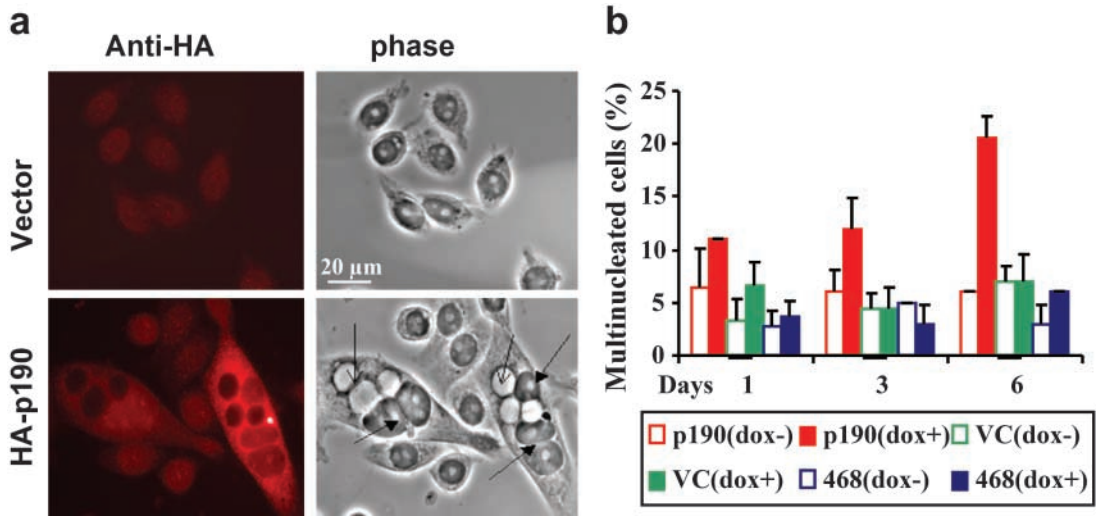

Figure 1. **p190 overexpression results in the multinucleation in MDA-MB-468 breast cancer cells.** (a) Immunofluorescence and phase contrast of a p190 overexpressor in the presence of Dox. (Bottom right) Open arrows, vacuoles; and closed arrows, nuclei. (b) Quantitation of the percent cells in clone 2413-6 that were multinucleated at indicated times of Dox treatment. 100 cells were counted in every treatment group and graphed using Microsoft Excel as the mean ± SD (n = 3).

contraction of cleavage furrow, both positive regulators (RhoGEFs) and negative regulators (RhoGAPs) of Rho are needed. A number of positive regulators of Rho, including ECT2 and VAV3 (Fujikawa et al., 2002), localize to the cleavage furrow, and cells lacking these RhoGEFs fail to recruit actin and other components into the cleavage furrow and are unable to undergo furrow ingression (Prokopenko et al., 1999; Bishop and Hall, 2000; Glotzer, 2001), demonstrating their importance. Microinjection of either RhoGDI or *Clostridium botulinum* C3 transferase, both potent Rho inhibitors, prevents the formation of the cleavage furrow in *Xenopus laevis* embryos (Kishi et al., 1993), HeLa cells (O'Connell et al., 1999), and T lymphocytes (Moorman et al., 1996). As discussed above, the Rho family GAP, mgcRacGAP, is critical for cleavage plane specification, but whether Rho-specific GAPs play a role in furrow specification site selection or contraction, especially in higher eukaryotes, is unclear.

p190RhoGAP (p190) is a multidomain protein (Settleman et al., 1992) that includes an NH_2-terminal GTP-binding domain (GBD), a middle domain (MD) with multiple protein–protein interaction motifs, and a COOH-terminal GAP domain. The GAP domain, with in vivo specificity for Rho GTPase (Ridley et al., 1993), plays a crucial role in regulating actin cytoskeletal rearrangements in axonal pathfinding and stability (Dupont and Blancq, 1999; Brouns et al., 2000, 2001; Billuart et al., 2001) and in response to growth factor stimulation (Chang et al., 1995a), integrin engagement (Nakahara et al., 1998; Arthur and Burridge, 2001), and v-Src transformation (Fincham et al., 1999). p190 is postulated to function as a negative regulator of Rho, enhancing the hydrolysis of active RhoGTP to inactive RhoGDP, which in turn is presumed to lead to an inactivation of RhoGTP effectors and ultimately actin stress fiber disassembly (Ridley et al., 1993; Chang et al., 1995a).

There are two distinct p190 proteins, p190A and p190B, encoded by different genes on different chromosomes. Germline expression of a NH_2-terminally truncated p190A RhoGAP (targeted disruption) results in premature death after birth, accompanied by defects in neural tube closure (Brouns et al., 2000, 2001; Billuart et al., 2001). A homozygous deletion of p190B results in reduced cell size, impaired insulin signaling, decreased adipogenesis and myogenesis (Sordella et al., 2002, 2003), and decreased incidence of mammary ductal morphogenesis (Chakravarty et al., 2003). Developmentally, p190B appears to function differently than p190A, although the phenotype of the homozygous null p190A mouse has not yet been reported. Only p190A (p190) will be discussed in this paper.

Other cellular processes in which p190A has been implicated include apoptosis and suppression of tumor growth. p190A's NH_2-terminal GTPase domain and COOH-terminal RhoGAP domain can independently suppress Ras-induced transformation in NIH3T3 cells (Wang et al., 1997). The p190A gene has been mapped to human chromosome 19q13.3, a region known to be rearranged in a variety of solid human tumors, including pancreatic carcinomas and gliomas (Tikoo et al., 2000), and p190A protein levels are up-regulated during apoptosis induced by castration of the prostate in rat models (Morrissey et al., 1999). In a mouse model, p190A inhibits PDGF-induced gliomas (Wolf et al., 2003). Due to these diverse effects of p190 on cell growth, we sought to define its mechanism of action.

Results

Overexpression of p190 induces formation of multinucleated cells

As our initial approach to investigate the consequences of overexpression of p190 on cell proliferation, we chose a tet-on conditional expression system. Fig. S1, available at http://www.jcb.org/cgi/content/full/jcb.200308007/DC1, shows that variable amounts of HA-tagged p190 protein were induced in different clones of MDA-MB-468 breast cancer cells

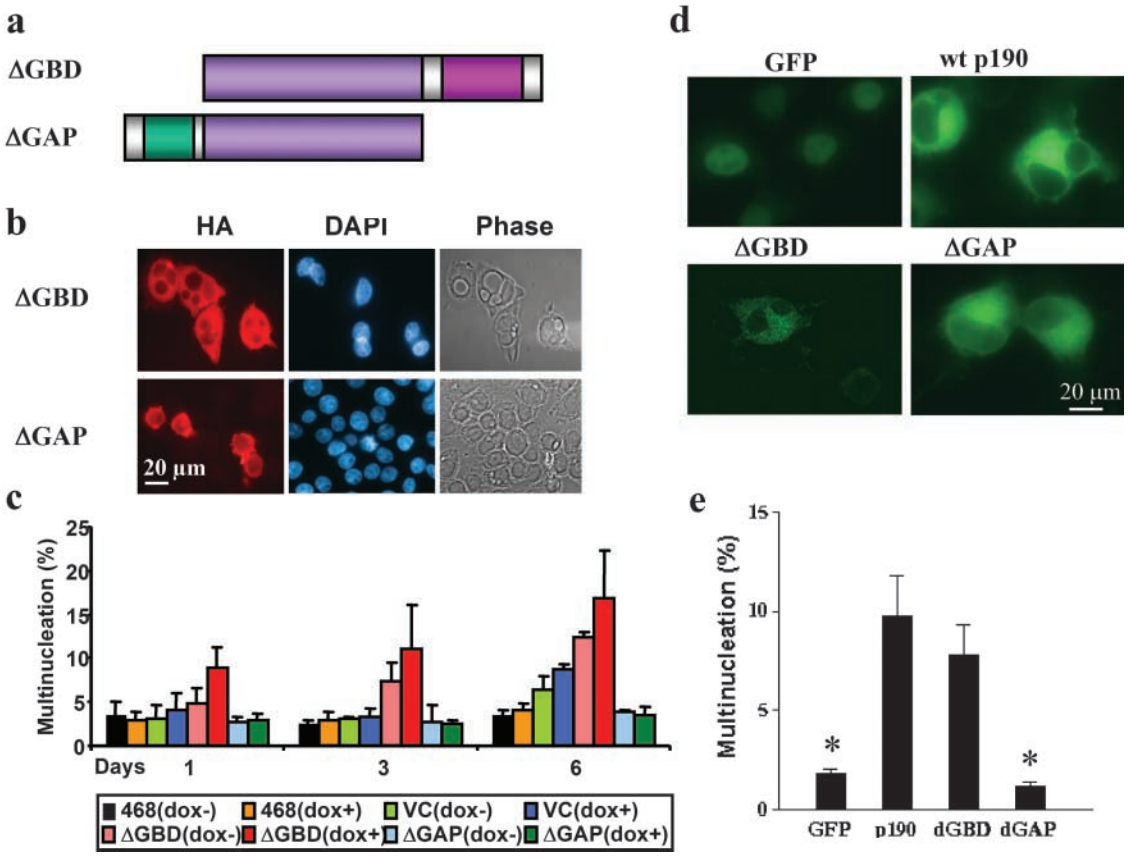

Figure 2. **The GAP domain of p190 is required for multinucleation.** (a) p190 constructs used in this work. (b) Immunofluorescence and phase contrast of ΔGBD and ΔGAP mutants overexpressed in 468 cells. Representative tet-on clones of ΔGBD and ΔGAP p190 were treated with 1 μg ml^{-1} Dox for 72 h and stained for HA-tagged ΔGBD and ΔGAP. (c) Quantitation of the percentage of HA positive cells that were multinucleated at day 1, 3, or 6 with 1 μg ml^{-1} Dox treatment. 100 cells were counted in every treatment group and graphed as the mean ± SD (n = 3). ΔGBD, GTP-binding domain deletion mutant; ΔGAP, GAP domain deletion mutant; VC, vector control; and 468, parental 468 cells. (d) Hela cells were transiently transfected with plasmids encoding HA-tagged wtp190, ΔGBD, ΔGAP, or GFP control vector. 24 h after transfection, cycling cells were examined by immunofluorescence for p190 expression and multinucleation. p190-expressing cells were scored positive for multinucleation based on DAPI and phase images. 100–150 cells were counted in every transfection group. (e) The percentage of multinucleation was quantitated using GraphPad Prism (n = 4) and graphed as the mean ± SEM. *, $P < 0.01$ relative to *wt* p190.

in a doxycycline (Dox) concentration– and time-dependent manner and that the maximum inducible level of p190 achieved was about twofold above the endogenous p190 level.

Fig. 1 a shows that Dox-induced overexpression of p190 resulted in the formation of giant cell bodies with abnormal vacuoles, and the presence of two or more nuclei per cell. Quantitative analysis (Fig. 1 b) revealed that p190 overexpression significantly increased the formation of multinucleated cells (~20%), compared with the vector control (7%) and parental MDA-MB-468 cells (5%), and that the number of nuclei increased with longer times of exposure to Dox (up to 6 d). Similar results were observed in different clones of tet-inducible p190 overexpressors. However, the magnitude of the effect was dependent on the level of expression of exogenous p190, as seen in different clones and in different cells within a clonal population. The multinucleated phenotype exhibited by p190 overexpressors suggested that p190 overexpression may block cytokinesis.

To determine which domain of p190 was responsible for the multinucleated phenotype, we generated GBD- and GAP-domain deletion constructs (ΔGBD and ΔGAP) of p190 in the MDA-MB-468 tet-on conditional expression system (Fig. 2 a). As with the full-length p190, ΔGBD and ΔGAP mutants were expressed only in the presence of Dox (unpublished data). Fig. 2 (b and c) shows that the ΔGAP-expressing cells failed to induce multinucleation, whereas the ΔGBD expressors developed multinucleated cells in comparable numbers (~17%) to those of *wt* p190 overexpressors (~20%). Similar results were obtained when HA-tagged *wt*, ΔGBD, and ΔGAP p190 encoding plasmids were transiently transfected into HeLa cells (Fig. 2, d and e). Multinucleation was also observed in C3H10T1/2 murine fibroblasts after transient overexpression of p190, suggesting that this phenomenon is not cell line– or type–specific and that the GAP domain is required for the multinucleated phenotype.

Localization of p190 to the cleavage furrow

Using confocal microscopy, we examined the subcellular localization of endogenous p190 in MDA-MB-468 cells at different stages of late mitosis, from anaphase to cytokinesis. Fig. 3 shows that endogenous p190 colocalized with cortical actin in the cellular membrane and appeared to concentrate in the cleavage furrow (as did actin) from the initial point of

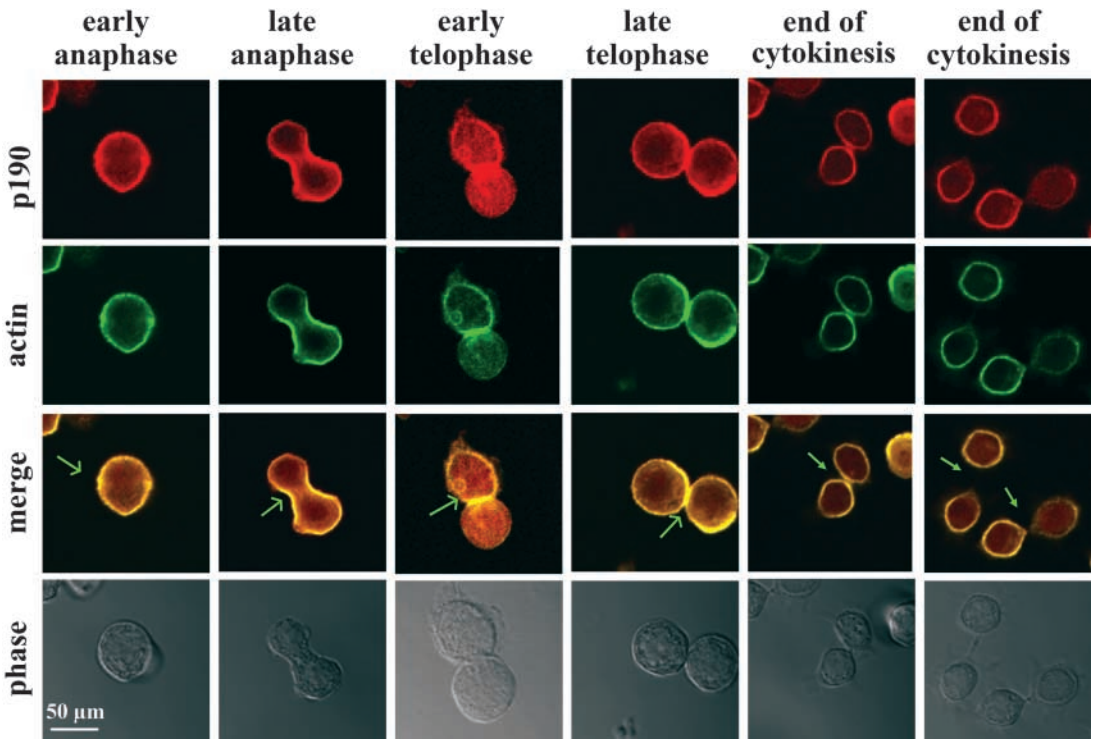

Figure 3. **Colocalization of endogenous p190 with actin to the cleavage furrow during cytokinesis.** Parental 468 cells were doubly arrested with thymidine and nocodazole and released from nocodazole for varying lengths of time up to 3 h. p190 and actin were visualized by fluorescence confocal microscopy using anti-p190 rabbit polyclonal antibody p27/Texas red–conjugated goat anti–rabbit IgG and FITC-phalloidin, respectively. Merged fluorescent and phase images are noted. Open arrows indicate cleavage furrow, and closed arrows indicate intercellular bridges.

furrow formation (furrow specification site) to the end of ring contraction. At the end of telophase, when the two daughter cells began to separate, p190 stained more diffusely. p190 was not detected in the midbody or in the intercellular bridge, although the latter structure could be seen clearly in phase contrast images. Endogenous p190 also colocalized with actin at the specification site of the cleavage furrow and in the contracting furrow of HeLa cells (Fig. S2, available at http://www.jcb.org/cgi/content/full/jcb.200308007/DC1). In cycling or serum-deprived 10T1/2 fibroblasts or 468 cells synchronized in the G1 phase of the cell cycle, p190 was diffusely scattered throughout the cytoplasm and did not exhibit predominant cortical actin colocalization (Chang et al., 1995a; unpublished data).

Abnormal cleavage furrow plane specification and defective furrow ingression upon overexpression of p190

Fig. 4 shows that overexpressed p190 also localized to the cleavage furrow, but surprisingly the positioning of furrow specification sites in many cells appeared to be aberrant, resulting in unequal cell division (note the cells that resemble budding yeast). Large, multilobed cells were also seen (Fig. 4). The genesis of these latter cells is consistent with multiple cleavage furrow initiation attempts (some of which appear to have been mislocalized) by a single cell and failure to complete contraction. These findings support the hypothesis that overexpressed p190 affects cleavage furrow plane specification and subsequent ring ingression.

Cell cycle–regulated expression of p190 in MDA-MB-468 human breast cancer cells

The effect of overexpression of p190 on cell growth suggested that the endogenous p190 protein level might be tightly controlled throughout the normal cell cycle. High experimental variation in immuno-detectable p190 levels from cycling cells (unpublished data) further supported this notion. To address this question, populations of MDA-MB-468 cells, blocked at G1, S, or M phases of the cell cycle, as well as at different stages of M phase (see Materials and methods), were examined by Western immunoblotting for levels of p190 protein. Flow cytometry verified that the synchronization process was successful (Fig. 5 a), and Fig. 5 b demonstrates by DAPI staining that the chromatin patterns were appropriate for each of the mitotic stages. Endogenous p190 protein level was found to be transiently reduced in late mitosis, with the lowest level being observed at 3 h after release from the nocodazole block (Fig. 5, c and d). This corresponds to the time when cells were undergoing cytokinesis. Normal p190 protein level was regained in G1. The decrease in p190 protein was also observed in HeLa cells, with the nadir occurring within 1 h upon release from nocodazole (as compared with 3 h in 468 cells; a difference likely due to more efficient synchronization in HeLa cells; Fig. S3, available at http://www.jcb.org/cgi/content/full/jcb.200308007/DC1). Finally, p190 protein was reduced by ~50% in a population of 468 cells blocked by double thymidine treatment and released for 10 h (DAPI staining indicated that the cells were in mitosis 9–11 h after release; unpublished data), suggesting that the decrease is not an artifact of nocoda-

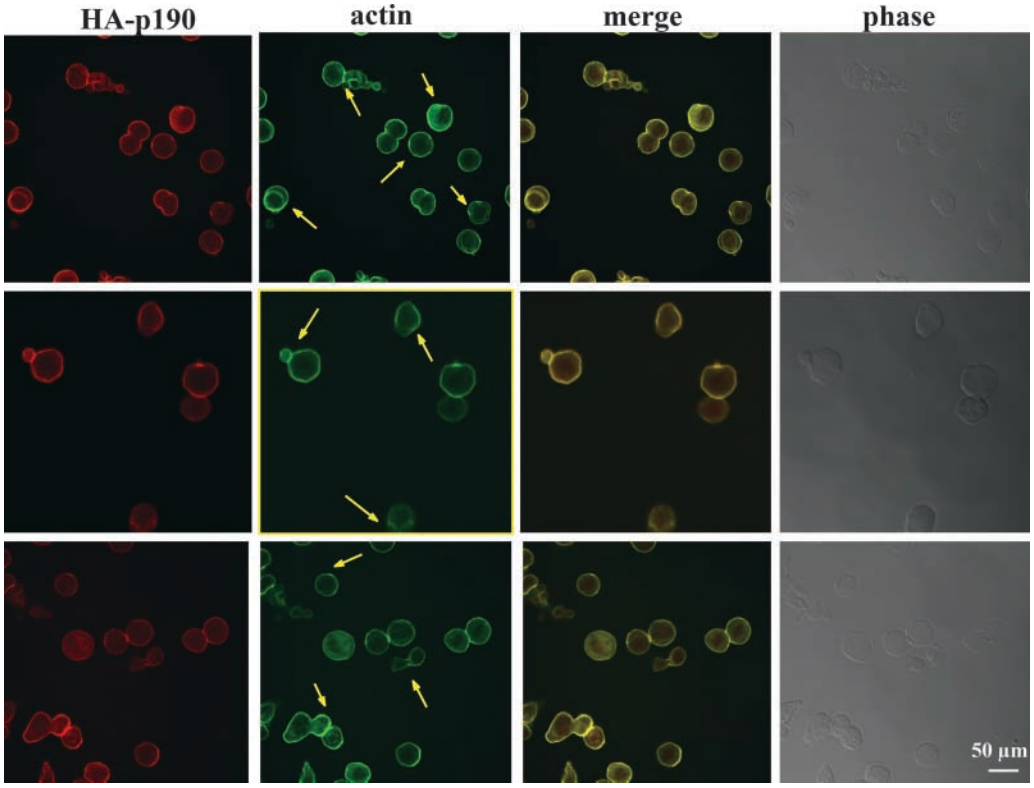

Figure 4. **Abnormal positioning of the cleavage furrow specification site, unequal daughter cell partitioning, and aberrant furrow contraction in cells overexpressing p190.** Dox-treated p190 overexpressing clone 2413-6 of 468 cells was doubly arrested with thymidine and nocodazole and released from the nocodazole block, as in Fig. 3. Cells were processed for immunofluorescent confocal microscopy as in Fig. 3, except that mAb HA11 and Texas red–conjugated goat anti–mouse IgG were used to detect HA-p190. Arrows indicate cleavage furrow specification sites.

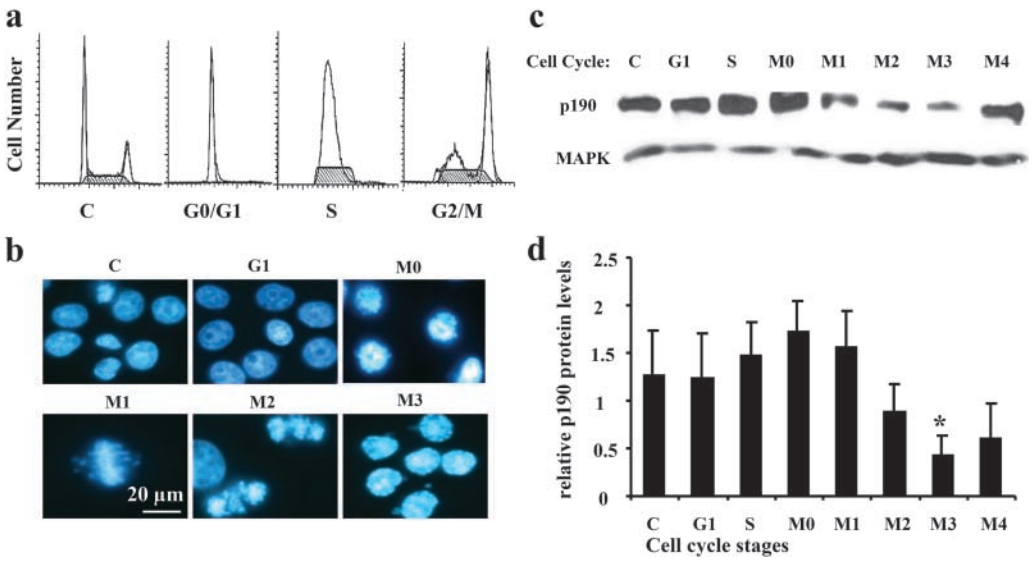

Figure 5. **Cell cycle–regulated levels of p190 protein in MDA-MB-468 cells.** (a) Flow cytometry analysis of 468 cells synchronized at different cell cycle stages. C represents cycling cells. G0/G1, S, and G2/M represent the population of cells in the G0/G1, S, and G2/M stages of the cell cycle, respectively. (b) Chromatin patterns of 468 cells synchronized at different stages of the cell cycle. C represents cycling cells. G1 represents cells in the G1 stage of the cell cycle that were synchronized by a double thymidine block. Cells in mitotic phase, obtained by nocodazole treatment (M0) and release from nocodazole for 45 min (M1), 90 min (M2), and 180 min (M3), were fixed and stained with DAPI. Chromatin patterns are consistent with cells in prometaphase (M0), metaphase (M1), anaphase (M2) and telophase/cytokinesis (M3). (c) Levels of endogenous p190 at different stages of the cell cycle. 100 μg of whole cell lysate from each cell cycle stage was immunoblotted with 8C10 (for p190) or the anti-Erk2 mAb (for MAPK as a loading control). (d) Quantitative analysis of multiple experiments represented by panel c. Each bar represents the relative protein level (densitometry of p190 level divided by loading control) and graphed as the mean ± SD ($n = 3$). Densitometry analysis was performed with Adobe Photoshop 4.0. M3 protein level is significantly different than the protein level in cycling cells. *, $P < 0.05$.

zole treatment. Together, these results indicate that the level of endogenous p190 protein is cell cycle regulated and undergoes a decrease in concordance with the onset of cytokinesis.

To determine whether overexpressed p190 was subjected to similar degradation, we examined levels of Dox-induced p190 (HA-tagged p190), as well as total p190 (overexpressed plus endogenous p190) in a tet-on inducible clone of MDA-MB-468 cells during cell cycle progression. Fig. 6 a depicts both HA-p190 and total p190 (HA-tagged p190 plus endogenous p190) levels throughout the cell cycle. In contrast to endogenous p190, quantitation of multiple experiments showed no significant reduction of total or HA-tagged p190 protein levels in late mitosis (Fig. 6 b). Similar results were obtained for different clones of p190 overexpressors when exogenous p190 was induced by Dox (unpublished data). The high levels of p190 in late mitosis correlated with the ability of overexpressed p190 to induce the multinucleated phenotype.

The reduction of p190 in late mitosis is regulated by ubiquitin-mediated degradation

Ubiquitin-mediated protein degradation via the 26S proteasome plays a key role in cell cycle progression. To investigate whether the reduced p190 protein levels observed in late mitosis were mediated by proteasome degradation, we analyzed the levels of endogenous p190 by Western immunoblotting in synchronized populations of cells that were treated with or without the proteasome inhibitor, MG132. Fig. 6 c shows that MG132 treatment maintained constant levels of p190 throughout all stages of the cell cycle, whereas p190 levels were decreased without MG132 treatment during later stages of mitosis. Quantitation of multiple experiments showed no significant reduction of p190 protein levels at the mitosis in the presence of MG132 (Fig. 6 d). The effect of MG132 treatment on endogenous p190 protein mimicked the result of p190 overexpression in the tet-on system. Although these results suggest that proteasome degradation may play a role in the regulation of endogenous p190 protein levels during the cell cycle, they are not necessarily an indication of direct degradation of p190 by the proteasome. The results could reflect an indirect effect on the levels of other cell cycle–regulated proteins (such as cyclins) and an inability to progress through mitosis. In fact, DAPI staining showed that MG132 induces mitotic arrest, even upon nocodazole withdrawal.

To test whether p190 is directly ubiquitinated, in vitro and in vivo ubiquitination works were performed. Fig. 7 a shows that in vitro–transcribed and –translated p190 was

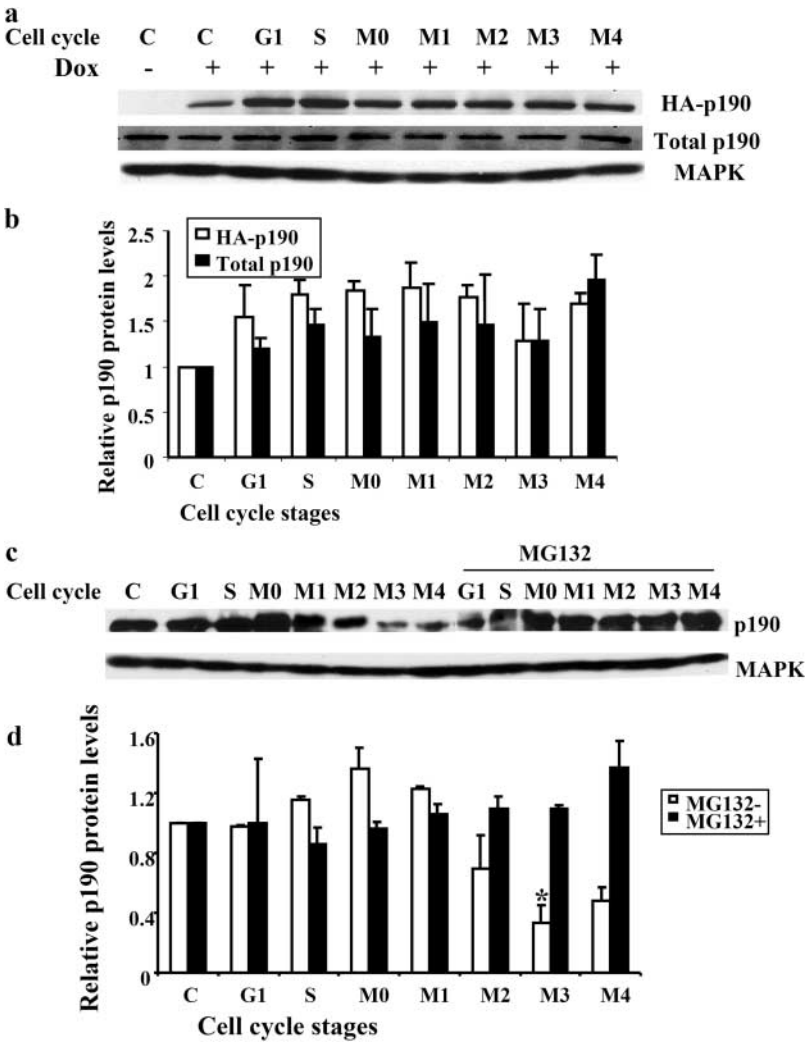

Figure 6. **Constitutive overexpression of p190 or the proteasome inhibitor, MG132, overcomes p190 degradation.** (a) p190 overexpression prevents its degradation at late mitosis. Clone 2413-6 was treated with 1 μg ml^{-1} Dox for 24 h and synchronized as in Fig. 5. 100 μg of lysate protein was subjected to Western immunoblotting by 12CA5 or 8C10 to detect HA-tagged p190 or total p190 levels, respectively. MAPK was blotted as a loading control. (b) Quantitation of panel a. Each bar represents the normalized protein level (densitometry units of p190 divided by loading control), relative to the ratio of cycling cells, which was set at one and graphed as the mean ± SD ($n = 3$). (c) Inhibition of p190 degradation by the proteasome inhibitor, MG132. Cells were synchronized as in Fig. 5 and left untreated or treated with 20 μM MG132. 100 μg of lysate protein was blotted for endogenous p190 protein levels, using mAb 8C10, or MAPK as a loading control. (d) Quantitation of panel c. Each bar represents the normalized protein level, relative to the ratio of cycling cells, which was arbitrarily set at one and graphed as the mean ± SD ($n = 3$). Densitometry analysis was performed using Adobe Photoshop 4.0. M3 protein level is significantly different than the protein level in cycling cells. *, $P < 0.05$.

ubiquitinated in the presence of exogenous ubiquitin and mitotic extracts prepared from 468 cells blocked in mitosis (M0) by nocodazole treatment or released from the nocodazole block for the indicated times. Ubiquitination is evidenced by the shift of p190 to higher molecular weight forms, some of which have just entered the gel. Significantly more ubiquitination was observed with M0 or M1.5 h release than with the 2.5- or 3-h release extracts (Fig. 7 b), thereby showing specificity for the process. The decrease in ubiquitination in the presence of methylated ubiquitin (M), which inhibits ubiquitin chain formation, also shows specificity of the reaction.

In vivo ubiquitination of p190 was analyzed in HeLa cells as described in Materials and methods. Immunoprecipates of p190, prepared from cells at different stages of mitosis plus or minus the specific proteasome inhibitor, lactacystin, contained proteins that were ubiquitinated in M0, as shown by anti-ubiquitin immunoblotting (Fig. 7 c). However, we were unable to detect laddering of p190 in the p190 blot of HeLa cells. Thus, using a different combination of antibodies, we tested whether p190 was directly ubiquitinated by immunoprecipitating p190 from 468 cells and subsequently immunoblotting the precipitated proteins with p190-specific antibodies (Fig. 7 d). A smeared banding pattern indicative of p190 ubiquitination in early mitotic samples, but not in cycling or late mitotic samples, was observed. As in the HeLa cells, the presence of lactacystin facilitated the appearance of ubiquitinated forms of p190. These findings suggest that p190 is directly ubiquitinated and that ubiquitination may play a role in the control of p190 protein level in mitosis. Different combinations of antibodies were needed (see Materials and methods and Fig. 7 for antibodies used) to detect p190 in the two cell lines (those used in HeLa cells functioned poorly in 468 cells and vice versa). The reason for this is not clear, but one explanation is that p190 may undergo differential posttranslational modification that results in epitope masking and inability to detect laddering in the p190 blot of HeLa cells.

To determine which domains of p190 are ubiquitinated during mitosis, cDNA plasmids encoding five distinct HA-tagged regions of p190 (representing the majority of the sequence of the protein) were generated and subjected to in vitro ubiquitination assays (using extracts from 468 cells blocked at mitosis), as described in Fig. 7. The regions analyzed included the NH_2-terminal GBD and COOH-terminal GAP domain, as well as sections 1–3 of the MD (Haskell et al., 2001). Fig. 8 a shows that the GBD is the most highly ubiquitinated region in mitosis, followed by section 1 and the GAP domain. Sections 2 and 3 sustained little to no ubiquitination in this analysis. This result indicated that the majority of p190 ubiquitination occurs in the GBD.

To determine the functional significance of ubiquitination, we asked which regions of p190 were critical for degradation. HA-tagged *wt*, ΔGBD, and ΔGAP p190 encoding plasmids were transiently expressed in HeLa cells, and the level of p190 was followed in cells arrested in mitosis and released for the indicated times. Fig. 8 (b and c) shows that *wt* and ΔGAP p190 are degraded in late mitosis, whereas ΔGBD is resistant to degradation within the same time frame. These results link ubiquitination of the GBD to degradation and suggest that the GTP binding region plays a key role in the regulation of p190 protein levels in late mitosis.

Discussion

Since its discovery, the molecular mechanism by which p190 regulates cell growth and death has remained elusive. Reasons for this are many fold. First, both overexpression (unpublished data) and underexpression (Fig. S4, available at http://www.jcb.org/cgi/content/ful/jcb.200308007/DC1) render cells inviable, thus limiting analysis of molecular events. Second, overexpressors score negatively for apoptotic markers (such as TUNEL) when cells are cultured in the presence of serum for up to 96 h, but ~30% are TUNEL positive in the absence of serum (as compared with

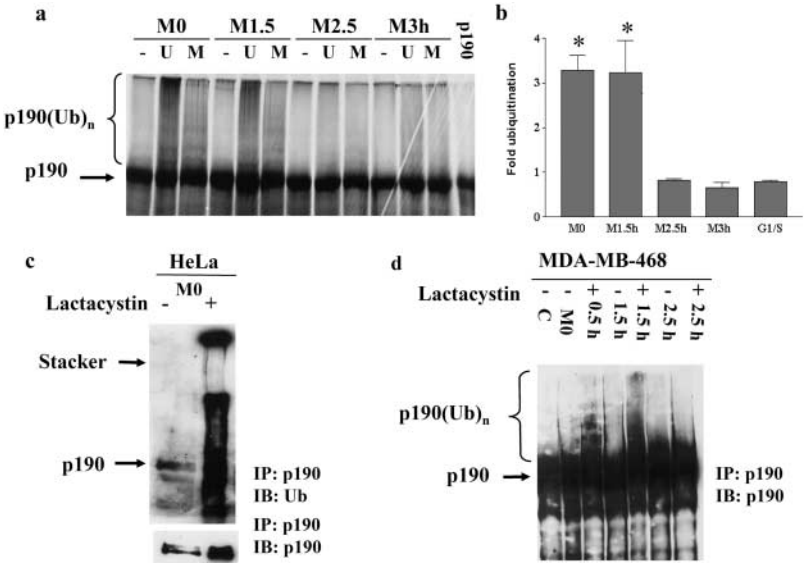

Figure 7. **In vitro and in vivo ubiquitination of p190.** (a) In vitro ubiquitination reactions using ^{35}S-labeled p190 and the mitotic extracts (M0, M1.5h, M2.5h, and M3h). −, the absence of exogenous ubiquitin in the reaction; M, methylated ubiquitin; and U, ubiquitin. The last lane is the in vitro ^{35}S-labeled p190 alone. p190(Ub)$_n$ denotes ubiquitinated p190. (b) Quantitation of multiple reactions are expressed as the mean ± SEM (*n* value ranging from three to seven experiments per extract). *, $P < 0.05$ for M0 and M1.5h compared to M2.5h, M3h, or G1/S. (c) In vivo ubiquitination of p190 in HeLa cells. HeLa cells were synchronized at different stages of mitosis with or without 10 μM of lactacystin, as described in Materials and methods. p190 was immunoprecipitated from 2 mg of lysate protein and blotted with anti-ubiquitin or anti-p190 antibodies. (d) In vivo ubiquitination of p190 in MDA-MB-468 cells. 468 cells were synchronized as in panel c, and p190 was immunoprecipitated from 2 mg of lysate using 8C10 and anti-p190 mAbs and immunoblotted with anti-p190 mAb.

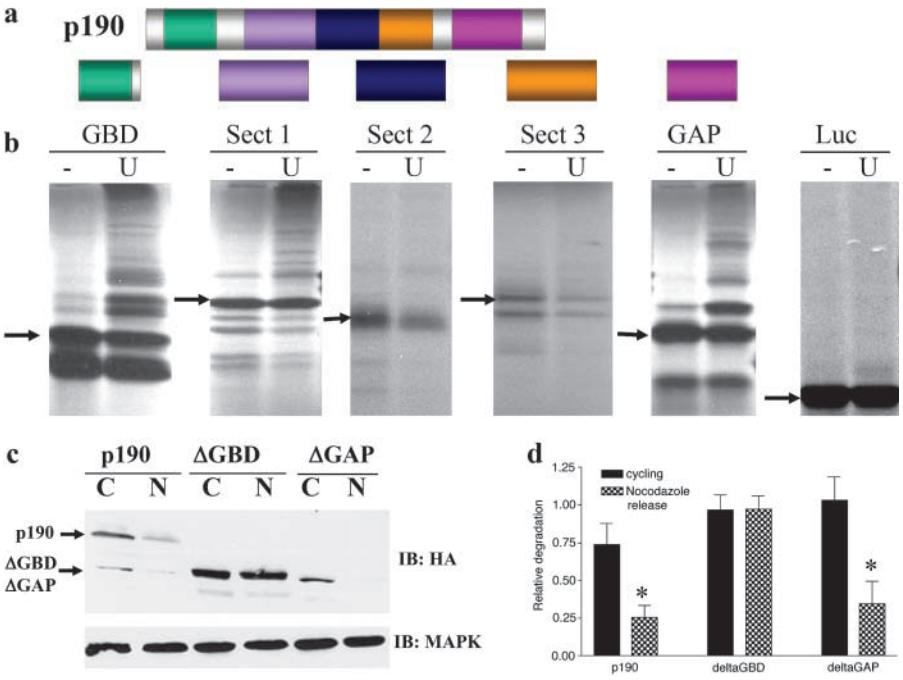

Figure 8. **The NH_2-terminal GBD of p190 is ubiquitinated and required for degradation of p190.** (a) Schematic representation of the p190 fragments subjected to the in vitro ubiquitination reaction in b. (b) In vitro ubiquitination of different p190 fragments. GBD, GTPase-binding domain; Sect 1, section 1 of the MD; Sect 2, section 2 of MD; Sect 3, section 3 of MD; GAP, GTPase-activating protein domain; and Luc, luciferase control. Arrows denote the translated protein without modification. (c) Degradation of exogenous p190 variants in HeLa cells. HeLa cells were transiently transfected with the indicated HA-tagged p190 expression plasmids. 24 h after transfection, cells were allowed to continue cycling (C) or treated with 40 ng/ml nocodazole (N) for 16 h, released from the block for 40 min, and lysed in RIPA buffer. 100 μg of whole cell lysate was immunoblotted with anti-HA mAb, 12CA5 or anti-MAPK B3B9 mAb as a loading control. (d) Quantitation of levels of p190 in cycling and mitotic HeLa cells. The ratio of p190 protein/MAPK from three to five independent experiments was quantified by AlphaEase software and graphed as the mean ± SEM. *, $P < 0.02$ relative to cycling cells expressing the same p190 variant.

5% of nonoverexpressors; unpublished data). This finding suggests that p190 overexpression predisposes cells to the apoptotic consequences of serum withdrawal but doesn't by itself cause apoptotic cell death. Third, p190 protein levels in breast and prostate cancer cell lines are not inversely correlated with the malignant phenotype, as would be expected of a classical tumor suppressor (unpublished data), although its GBD and GAP domain reverse Ras-induced NIH3T3 cell transformation (Wang et al., 1997). Fourth, our findings that p190 appears to be required for progression through the earlier stages of the cell cycle (Chang et al., 1995a; Fig. S4) and is detrimental in the late stages of the cell cycle when overexpressed (Fig. 4) suggest that it has both positive and negative regulatory roles to play in cell cycle progression. From these analyses, we hypothesize that the level of p190 protein is critical for maintaining cell homeostasis and progression through the cell cycle, notably in late mitosis where a transient reduction is associated with successful completion of the process.

At what point in cytokinesis are levels of p190 most critical? Although it has been well established that the mitotic spindle is critical for cleavage furrow initiation, recent data suggest that two independent pathways, centrosome separation and central spindle assembly, trigger cleavage furrow initiation by generating a low microtubule density area near the site of furrow formation (Dechant and Glotzer, 2003). These actions appear to be coordinated with Rho, as described in the Introduction. Our findings that both endogenous and ectopically expressed p190 localize to cleavage furrow specification sites and that overexpression of p190 results in abnormal plane specification (Fig. 4) further support the critical involvement of Rho in furrow initiation and formation, and identify another potentially important regulator of Rho (p190) in this process as well. Exactly how p190 interdigitates with the known regulators of cleavage furrow plane specification is unclear at the present time (Gonzalez, 2003) and awaits identification of p190 binding partners.

The presence of p190 in the cleavage furrow throughout the contraction process suggests that furrow ingression is also dependent on a critical level of active Rho. Indeed, Pelham and Chang (2002) recently showed that the contractile ring is a dynamic structure, in which actin and other components continuously assemble and disassemble during furrow contraction. Because Rho and its regulators are key modulators of actin assembly and disassembly, the localization of Rho GEFs and GAPs in the furrow along with Rho supports the idea that these molecules are important to the continual rearrangements that the contractile ring undergoes during furrow ingression.

However, little to no endogenous p190 can be detected in the midbody or intercellular bridge, which forms just before the completion of cytokinesis (Fig. 3). This structure is assembled between the newly forming daughter cells as the actomyosin contractile ring comes into close proximity to the central spindle. The absence of p190 from this structure could be due to the poor penetrance of antibodies into these structures, thus preventing a definitive interpretation of the results. Alternatively, if p190 is truly absent from these structures, such a result would suggest that p190 is not a critical regulator of Rho during this phase of cytokinesis, although Rho family members have been linked to these late stages of the process. Other Rho family GAPs have also been implicated as critical regulators of midbody formation, including CYK-4 in *C. elegans* and its

human orthologue, mgcRacGAP (Jantsch-Plunger et al., 2000; Hirose et al., 2001).

The requirement for the GAP domain of p190 to induce the multinucleated phenotype (Fig. 2) suggests that a critical role of p190 in cytokinesis is to regulate Rho activity by modulating the level of RhoGTP. Endogenous p190 levels are in fact transiently decreased in late mitosis when cytokinesis takes place (Fig. 5), suggesting that elevated RhoGTP levels are needed to traverse this stage of mitosis. We speculate that constitutive overexpression of p190 results in reduced RhoGTP levels, thereby causing abnormal cleavage furrow formation and perhaps ineffective furrow contraction. Indeed, Maddox and Burridge (2003) have reported that RhoGTP levels are elevated during normal mitosis, supporting the notion that high RhoGTP (and low RhoGAP activity) is associated with completion of mitosis. By using FRET-based probes, Yoshizaki et al. (2003) found that elevated RhoGTP specifically localizes to the cleavage furrow in late cytokinesis, whereas RacGTP partitions to the spindle poles, and Cdc42GTP is diffusely distributed throughout the cells. Thus, high levels of RhoGTP occur in the same time and place that we observe a reduction in p190 protein levels and, concurrently, a decrease in RhoGAP activity. That p190 activity may be specifically affecting RhoGTP levels in the cleavage furrow and not RacGTP or Cdc42GTP levels is consistent with RhoGTP being the preferred substrate (vs. Rac and Cdc42) for p190 in vivo (Ridley et al., 1993).

Our finding that gene silencing of p190A results in reduced viability and highly adhesive and thinly spread cells that fail to accumulate in mitosis upon nocodazole treatment (Fig. S4) suggests that too much RhoGTP can also be detrimental to cell cycle progression. The absence of a cytokinetic defect in the p190A-targeted disruption mouse (Brouns et al., 2000, 2001) or in the p190B knockout mouse (Sordella et al., 2002) appears to conflict with our findings. However, potential compensatory mechanisms by other RhoGAPs during development in knockout animals make interpretation of the phenotypes (or lack thereof) more problematic. An additional complication is that there may be some functional redundancy among Rho family GAPs with regard to cytokinesis (e.g., mgcRacGAP). Finally, if p190 needs to be degraded (or expression reduced) for cytokinesis to occur, a knockout or knockdown might not exhibit a phenotype. Thus, in light of these considerations and the results of our gene silencing experiments, our best tool to date in understanding the role of p190 in cytokinesis has been the overexpression strategy.

Our data show that multinucleation is accompanied by large vacuoles in p190 overexpressors. These abnormal vacuoles may be caused by perturbation of vesicle transport or membrane vesicle fusion systems of the cell. Recent data suggest that membrane vesicle transport to and fusion at the site of cleavage is required for proper completion of cytokinesis (Straight and Field, 2000; Finger and White, 2002). A microtubule structure, known as the furrow microtubule array, is required for directing membrane vesicles to the site of the cleavage furrow (Danilchik et al., 1998; Straight and Field, 2000). Because it is unclear whether p190 localizes to the midbody (Fig. 3), where substantial membrane deposition occurs in late cytokinesis, it is possible that p190 plays a role in membrane recruitment at earlier stages of cytokinesis. Because p190 is a multidomain protein, it could induce multinucleation and vacuole formation by independent mechanisms that involve distinct domains, in addition to its GAP domain. Support for this notion comes from several reports. Not only is there evidence showing possible involvement of p190 in the endocytosis of the EGF receptor (Wang et al., 1996), but its associated protein, p120RasGAP, has also been shown to regulate vesicular transport to the Golgi apparatus (Kulkarni et al., 2000). In addition, the GTPase domain in the NH_2 terminus of p190 contains motifs that are closely related to the small G protein, Ypt2, in yeast (Foster et al., 1994). Ypt (Rab) family proteins are known to regulate vesicular transport (Haubruck et al., 1990). Recent data also suggest that c-Src tyrosine kinase may participate in the process of cytokinesis. c-Src is associated and colocalized with the diaphanous-related formins, which are Rho GTPase-binding proteins, in endosomes and in midbodies of dividing cells (Tominaga et al., 2000). Because p190 is a substrate of c-Src (Chang et al., 1995a; Roof et al., 1998; Brouns et al., 2001), it is possible that c-Src plays a role in p190-induced regulation of cytokinesis. Thus, disturbance of membrane vesicle transport may also contribute to the p190-induced block in cytokinesis. Further experiments are needed to identify the origin of the vacuoles in p190 overexpressors and their potential role in cytokinesis.

The ubiquitination works depicted in Fig. 7 suggest that p190 is a target of ubiquitin-mediated degradation in late mitosis. In further support of its regulated degradation, protein sequence analysis indicates that p190 contains seven potential ubiquitination motifs, including five destruction boxes (D-boxes) and two KEN-boxes. The D-box is a well-characterized ubiquitination motif found in most mitotic cyclins (King et al., 1996). The consensus sequence of the D-box, RXXL, is found at residues 346, 833, 872, 903, and 1216 of p190. KEN-boxes (Pfleger and Kirschner, 2000) are found in the GAP domain (residues 1366–1369) and the NH_2-terminal portion of the MD (residues 437–439) of p190. Both motifs are recognized by an ubiquitin E3 ligase, the anaphase promoting complex (Pfleger and Kirschner, 2000) which is active from metaphase to G1. Several other candidate E3 ligases, like Skp1–cullin–F-box complex and Chfr (Peters, 1998; Kang et al., 2002), may mediate the ubiquitination of p190 during mitosis and need to be investigated.

An analysis of the time courses of ubiquitination versus degradation raises the question of why the steady-state level of p190 decreases only upon exit from M phase, if the highest ubiquitination activity is in early mitosis. Fig. 7 b shows that the highest ubiquitinating activity was found in M0 extracts and in M1.5 h extracts (released from nocodazole in the absence of MG132 for 1.5 h). Fig. 6 c shows that degradation was apparent in intact cells 2 h after release and that the nadir of p190 levels was reached at 3 h after release. We interpret these results to mean that p190 could be ubiquitinated anytime from the moment of entrance into mitosis through 1.5 h into the process and degraded within 1.5–3 h afterwards. Whether this means that selected p190 molecules are ubiquitinated and degraded rapidly at specific time

intervals or whether there is a delay between ubiquitination and degradation of the entire degradable population is a subject requiring further investigation.

The structure–function analysis depicted in Fig. 8 shows that the GTP binding region is important for both ubiquitination and degradation of p190 during mitosis. The ΔGBD variant represents a nondegradable form of p190 that induces multinucleation when overexpressed transiently in HeLa cells or in the tet-on inducible system in 468 cells (Fig. 2), linking high levels of nondegradable p190 to disruptions in cytokinesis. These results suggest that the GBD may function as an autoregulator of endogenous p190 protein level in late mitosis by controlling ubiquitination-mediated degradation. This conclusion is consistent with a previous report demonstrating that the GBD controls p190 activity (Tatsis et al., 1998). However, a discordance in the data is revealed by the analysis of full-length p190, where degradation of the protein was observed in the transient transfectants (Fig. 8), but not in the tet-on inducible 468 clones (Fig. 6), yet both overexpression methods resulted in a multinucleated phenotype (Figs. 1 and 2). These results could be interpreted in several ways. On one hand, the discordance may only reflect differences in the overexpression systems, where the constantly elevated level of p190 in the presence of Dox may overwhelm the degradation pathway, resulting in high levels of p190, whereas the short-lived, elevated levels in the transient expression system are more readily proteolyzed. With such considerations, the hypothesis that degradation of endogenous p190 is required for successful completion of cytokinesis remains valid. On the other hand, it is possible that resistance to ubiquitination-mediated degradation is not required for overexpressed p190 to induce multinucleation and that ubiquitination/degradation of endogenous p190 may regulate another process not critical to completion of cytokinesis. In any event, the data in both overexpression systems reveal a critical need for the RhoGAP domain for the effects of p190 overexpression on cytokinesis and clearly link p190 to this process. This hypothesis is further supported by the fact that RhoGTP levels are elevated during cytokinesis (Yoshizaki et al., 2003) when we observe a decrease in p190 protein level.

Together, the results in this paper suggest that p190 can affect cytokinesis through its GAP domain by regulating Rho activity and that this function is controlled by the GTP binding region through ubiquitination and degradation of p190. This regulated degradation may be important for completion of cytokinesis. From this perspective, p190 may act as a regulator of late mitosis (perhaps even at a secondary or tertiary level) to ensure that cells progress through cytokinesis normally.

Materials and methods

Tissue culture

MDA-MB-468 human breast cancer cells were cultured in DME (GIBCO BRL) with 5% FBS and antibiotics. Murine C3H 10T1/2 fibroblasts and HeLa cells were cultured in DME with 10% serum and antibiotics.

Immunofluorescence

Cells were prepared for immunofluorescence as described in Chang et al. (1995b), except that 2 μg ml^{-1} anti-HA mAb, HA11 (BabCO), and 1 μg ml^{-1} Texas red–conjugated goat anti–mouse IgG (Jackson ImmunoResearch Laboratories, Inc.) were used for staining HA-p190. Endogenous p190 was stained with anti-p190 mAb, 8C10, or polyclonal rabbit antibody p27 (derived and characterized in our laboratory; Chang et al., 1995a, b) as the primary antibodies. For actin localization, cells were incubated with 5 U ml^{-1} FITC-labeled phalloidin (Molecular Probes Inc.) in PBS for 1 h nuclear DNA was stained with 2 μg ml^{-1} DAPI (Sigma-Aldrich) in PBS for 3 min. Coverslips were mounted on microscope slides and cells were viewed on a confocal microscope (model Pascal; Carl Zeiss MicroImaging, Inc.).

HeLa cells were transfected with p190 variants using Polyfect (QIAGEN) according to the manufacturer's instructions. Cells were fixed and stained as above 24 h after transfection using 2.5 μg/ml anti-HA FITC (Roche), and viewed on a fluorescent microscope (model Orthoplan; E. Leitz, Inc.).

Western blotting

Cells were grown to ~90% confluence at 37°C,lysed, and subjected to Western blotting as described previously (Chang et al., 1995a), using the following primary antibodies (1 μg ml^{-1} in blocking buffer): anti-HA mAb, 12CA5 (BabCO) for HA-tagged p190; 8C10 mAb for endogenous p190; and mAb B3B9 for MAPK (a gift of M. Weber, University of Virginia, Charlottesville, VA). Membranes were incubated with HRP-conjugated anti–mouse IgG secondary antibody (1:5,000; Amersham Biosciences), and visualized by ECL (ECL™; Amersham Biosciences). Results were quantified by densitometric analysis using Adobe Photoshop 4.0.

Generation of MDA-MB-468 tet-on p190-inducible cell lines

The tet-on expression system obtained from CLONTECH Laboratories, Inc. was used according to the manufacturer's directions. The HindIII–EcoRV fragments from HA-tagged wild-type p190-A (Rc190-wt) (Settleman et al., 1992) were inserted into the pTRE-2 vector, respectively, to yield pTRE190A. HA-tagged ΔGBD (amino acids 379–1514) and ΔGAP (amino acids 1–1180) were cloned into the pTRE-2 vector by PCR. The constructs were verified by DNA sequencing. Clones of 468 cells were stably transfected with pTet-on, selected in 800 μg ml^{-1} G418, and screened for >100-fold Dox inducibility and low background after transient transfection with the pTRE2-Luc plasmid. Double-stable cell lines were generated by cotransfecting pTet-on stable clone with pTRE-p190 constructs above together with pBabe (puromycin) at a ratio of 10:1, respectively, and selected with 400 μg ml^{-1} G418 and 250 ng ml^{-1} puromycin in tissue culture medium.

Cell cycle synchronization and flow cytometry

Cell cycle–synchronized cells were obtained by treatment with 2 mM thymidine (Sigma-Aldrich) in tissue culture medium for 12–16 h; cells were washed and incubated in normal medium for 8–10 h to release them from the block. Cells treated in this manner were further enriched for G1/S, S, and M phases by the following treatments: G1/S phase (400 μM L-minosine [Sigma-Aldrich] for 12–16 h); S phase (2 mM thymidine for 12–16 h, washed, and replaced with normal medium for 4 h); and M phase (40 ng ml^{-1} nocodazole [Sigma-Aldrich] for 12–16 h). M phase cells were washed in PBS and released from the nocodazole block by addition of fresh medium (45–240 min). MG132 (Sigma-Aldrich) at 20 μM was added during the release from nocodazole for some experiments. Cells were fixed and stained with DAPI, or prepared for flow cytometry by trypsinization, washing in PBS, fixation in 90% ethanol for 1 h at 4°C, and washing again in PBS. DNA was labeled with 50 μg ml^{-1} propidium iodide (Sigma-Aldrich) in PBS containing 25 μg ml^{-1} RNase A for 30 min at 37°C in the dark. Stained cells were sorted and analyzed in the FACS Core Facility at the University of Virginia.

In vitro ubiquitination

In vitro ubiquitination reactions were performed as described previously (Cockman et al., 2000). The energy regenerating system, methylated ubiquitin, and ubiquitin aldehyde were purchased from Boston Biochem, Inc. p190A mutants, including the isolated GBD (amino acids 1–266), section 1 (amino acids 379–646), section 2 (amino acids 647–918), and section 3 (amino acids 919–1183) of the MD, and the RhoGAP domain (amino acids 1260–1469) were cloned into the pKH3 plasmid (a gift from I. Macara, University of Virginia), using BamHI and EcoRI restriction digestions. All constructs including luciferase as a negative control were in vitro–transcribed and –translated from the plasmids in the presence of 20 μCi [^{35}S]methionine (1,175 Ci $mmol^{-1}$; Amersham Biosciences) using TnT Quick Coupled Reticulocyte Lysate Transcription/Translation Systems

(Promega). Products of the reaction were analyzed by 7% SDS-PAGE and autoradiography after treatment of the gels with Amplify reagent (Amersham Biosciences). Densitometric analysis of [^{35}S]-bands was accomplished with ImageQuant, whereas GraphPad Prism was used for statistical analysis and graphing. For quantitation of the experiments, the area of the lane above the translated protein containing ubiquitinated p190 was divided by the area above the translated protein alone. The ratio is graphed as fold ubiquitination.

In vivo ubiquitination

HeLa cells were synchronized in mitosis with lactacystin (a proteasome inhibitor; Calbiochem) added at the time of release from nocodazole. Cells were lysed in RIPA-p-Tyr lysis buffer containing 50 mM NEM (Sigma-Aldrich) and 10 μM lactacystin. 2 mg of clarified extract was immunoprecipitated as described previously (Chang et al., 1995a) with a combination (3 μg each) of anti-p190 (Transduction Laboratories) and 3D4 (Chang et al., 1995b) mAbs. Precipitated proteins were separated on 7% SDS-PAGE and immunoblotted with rabbit p27 anti-p190 polyclonal antibody (Chang et al., 1995b) or ubiquitin mAb (Santa Cruz Biotechnology, Inc.) at 1:1,000 and 1:100 dilutions, respectively. Immune complexes were detected with HRP-conjugated anti–rabbit or anti–mouse IgG (Amersham Biosciences) and Femto reagent (Pierce Chemical Co.). Images were captured using AlphaInnotech software. MDA-MB-468 cells were synchronized and lysed as above. Anti-p190 (Transduction Laboratories) and 8C10 (Chang et al., 1995b) mAbs were used for immunoprecipitation, and the anti-p190 mAb (Transduction Laboratories) was used for Western blotting. Membranes were incubated with secondary antibody and visualized by ECL.

Degradation assay

HeLa cells were transfected with the indicated 1–3 μg HA-tagged p190 plasmids using Polyfect per 100-mm tissue culture dish. 24 h after transfection, one of two duplicate dishes was incubated with 40 ng/ml nocodazole for 16 h, washed repeatedly to remove the nocodazole, replenished with fresh medium, and allowed to progress through mitosis for 40 min at 37°C. The control dish was maintained as an asynchronously cycling population. Cells were lysed using RIPA buffer, and 100 μg of lysate protein was separated by 7% SDS-PAGE and subjected to Western immunoblotting as described in the Western blotting section. Densitometric analysis using AlphaEase software was performed to obtain the ratios of p190/MAPK protein, and the values were graphed using GraphPad.

Online supplemental material

Fig. S1 shows the variable amounts of tet-inducible overexpression of HA-tagged p190 in different clones of MDA-MB-468 breast cancer cells and the dose and time analysis of this overexpression. Figs. S2 and S3 show that endogenous p190 localizes to the cleavage furrow with actin and is degraded during mitosis in HeLa cells, similar to its localization and degradation in 468 cells. Fig. S4 shows the phenotype induced by gene silencing of p190A in 468 cells. Online supplemental materials are available at http://www.jcb.org/cgi/content/full/jcb.200308007/DC1.

We thank W. Ross for flow cytometry analysis, L. Palmer for her assistance with the in vitro ubiquitination assays, I. Macara for the HA-tagged GBD in the PKH3 expression plasmid, and T. Stukenburg for critical reading of the manuscript. We are also grateful to the S.J. Parsons laboratory and the Parsons/Weber/Parsons group for helpful discussions.

This work was supported by grant CA39438 from the National Cancer Institute.

Submitted: 4 August 2003
Accepted: 29 September 2003

References

Arthur, W.T., and K. Burridge. 2001. RhoA inactivation by p190RhoGAP regulates cell spreading and migration by promoting membrane protrusion and polarity. *Mol. Biol. Cell.* 12:2711–2720.

Billuart, P., C.G. Winter, A. Maresh, X. Zhao, and L. Luo. 2001. Regulating axon branch stability: the role of p190 RhoGAP in repressing a retraction signaling pathway. *Cell.* 107:195–207.

Bishop, A.L., and A. Hall. 2000. Rho GTPases and their effector proteins. *Biochem. J.* 348:241–255.

Bonaccorsi, S., M.G. Giansanti, and M. Gatti. 1998. Spindle self-organization and cytokinesis during male meiosis in asterless mutants of *Drosophila melanogaster*. *J. Cell Biol.* 142:751–761.

Brouns, M.R., S.F. Matheson, K.Q. Hu, I. Delalle, V.S. Caviness, J. Silver, R.T. Bronson, and J. Settleman. 2000. The adhesion signaling molecule p190 RhoGAP is required for morphogenetic processes in neural development. *Development.* 127:4891–4903.

Brouns, M.R., S.F. Matheson, and J. Settleman. 2001. p190 RhoGAP is the principal Src substrate in brain and regulates axon outgrowth, guidance and fasciculation. *Nat. Cell Biol.* 3:361–367.

Chakravarty, G., D. Hadsell, W. Buitrago, J. Settleman, and J.M. Rosen. 2003. p190-B RhoGAP regulates mammary ductal morphogenesis. *Mol. Endocrinol.* 17:1054–1065.

Chang, J.H., S. Gill, J. Settleman, and S.J. Parsons. 1995a. c-Src regulates the simultaneous rearrangement of actin cytoskeleton, p190RhoGAP, and p120RasGAP following epidermal growth factor stimulation. *J. Cell Biol.* 130:355–368.

Chang, J.H., W.M. Sutherland, and S.J. Parsons. 1995b. Monoclonal antibodies to oncoproteins. *Methods Enzymol.* 254:430–445.

Cockman, M.E., N. Masson, D.R. Mole, P. Jaakkola, G.W. Chang, S.C. Clifford, E.R. Maher, C.W. Pugh, P.J. Ratcliffe, and P.H. Maxwell. 2000. Hypoxia inducible factor-alpha binding and ubiquitylation by the von Hippel-Lindau tumor suppressor protein. *J. Biol. Chem.* 275:25733–25741.

Danilchik, M.V., W.C. Funk, E.E. Brown, and K. Larkin. 1998. Requirement for microtubules in new membrane formation during cytokinesis of *Xenopus* embryos. *Dev. Biol.* 194:47–60.

Dechant, R., and M. Glotzer. 2003. Centrosome separation and central spindle assembly act in redundant pathways that regulate microtubule density and trigger cleavage furrow formation. *Dev. Cell.* 4:333–344.

Dupont, H., and M. Blancq. 1999. Formation of complexes involving RasGAP and p190 RhoGAP during morphogenetic events of the gastrulation in *Xenopus*. *Eur. J. Biochem.* 265:530–538.

Fincham, V.J., A. Chudleigh, and M.C. Frame. 1999. Regulation of p190 RhoGAP by v-Src is linked to cytoskeletal disruption during transformation. *J. Cell Sci.* 112:947–956.

Finger, F.P., and J.G. White. 2002. Fusion and fission: membrane trafficking in animal cytokinesis. *Cell.* 108:727–730.

Foster, R., K.Q. Hu, D.A. Shaywitz, and J. Settleman. 1994. p190 RhoGAP, the major RasGAP-associated protein, binds GTP directly. *Mol. Cell. Biol.* 14: 7173–7181.

Fujikawa, K., Y. Inoue, M. Sakai, Y. Koyama, S. Nishi, R. Funada, F.W. Alt, and W. Swat. 2002. Vav3 is regulated during the cell cycle and effects cell division. *Proc. Natl. Acad. Sci. USA.* 99:4313–4318.

Glotzer, M. 2001. Animal cell cytokinesis. *Annu. Rev. Cell Dev. Biol.* 17:351–386.

Gonzalez, C. 2003. Cell division: the place and time of cytokinesis. *Curr. Biol.* 13: R363–R365.

Haskell, M.D., A.L. Nickles, J.M. Agati, L. Su, B.D. Dukes, and S.J. Parsons. 2001. Phosphorylation of p190 on Tyr1105 by c-Src is necessary but not sufficient for EGF-induced actin disassembly in C3H10T1/2 fibroblasts. *J. Cell Sci.* 114:1699–1708.

Haubruck, H., U. Engelke, P. Mertins, and D. Gallwitz. 1990. Structural and functional analysis of ypt2, an essential ras-related gene in the fission yeast *Schizosaccharomyces pombe* encoding a Sec4 protein homologue. *EMBO J.* 9:1957–1962.

Hirose, K., T. Kawashima, I. Iwamoto, T. Nosaka, and T. Kitamura. 2001. MgcRacGAP is involved in cytokinesis through associating with mitotic spindle and midbody. *J. Biol. Chem.* 276:5821–5828.

Jantsch-Plunger, V., P. Gonczy, A. Romano, H. Schnabel, D. Hamill, R. Schnabel, A.A. Hyman, and M. Glotzer. 2000. CYK-4: a Rho family gtpase activating protein (GAP) required for central spindle formation and cytokinesis. *J. Cell Biol.* 149:1391–1404.

Kang, D., J. Chen, J. Wong, and G. Fang. 2002. The checkpoint protein Chfr is a ligase that ubiquitinates Plk1 and inhibits Cdc2 at the G2 to M transition. *J. Cell Biol.* 156:249–259.

King, R.W., M. Glotzer, and M.W. Kirschner. 1996. Mutagenic analysis of the destruction signal of mitotic cyclins and structural characterization of ubiquitinated intermediates. *Mol. Biol. Cell.* 7:1343–1357.

Kishi, K., T. Sasaki, S. Kuroda, T. Itoh, and Y. Takai. 1993. Regulation of cytoplasmic division of *Xenopus* embryo by rho p21 and its inhibitory GDP/GTP exchange protein (rho GDI). *J. Cell Biol.* 120:1187–1195.

Kulkarni, S.V., G. Gish, P. van der Geer, M. Henkemeyer, and T. Pawson. 2000. Role of p120 Ras-GAP in directed cell movement. *J. Cell Biol.* 149:457–470.

Maddox, A.S., and K. Burridge. 2003. RhoA is required for cortical retraction and

rigidity during mitotic cell rounding. *J. Cell Biol.* 160:255–265.

Moorman, J.P., D.A. Bobak, and C.S. Hahn. 1996. Inactivation of the small GTP binding protein Rho induces multinucleate cell formation and apoptosis in murine T lymphoma EL4. *J. Immunol.* 156:4146–4153.

Morrissey, C., S. Bennett, E. Nitsche, R.S. Guenette, P. Wong, and M. Tenniswood. 1999. Expression of p190A during apoptosis in the regressing rat ventral prostate. *Endocrinology.* 140:3328–3333.

Nakahara, H., S.C. Mueller, M. Nomizu, Y. Yamada, Y. Yeh, and W.T. Chen. 1998. Activation of beta1 integrin signaling stimulates tyrosine phosphorylation of p190RhoGAP and membrane-protrusive activities at invadopodia. *J. Biol. Chem.* 273:9–12.

O'Connell, C.B., S.P. Wheatley, S. Ahmed, and Y.L. Wang. 1999. The small GTP-binding protein rho regulates cortical activities in cultured cells during division. *J. Cell Biol.* 144:305–313.

Pelham, R.J., and F. Chang. 2002. Actin dynamics in the contractile ring during cytokinesis in fission yeast. *Nature.* 419:82–86.

Peters, J.M. 1998. SCF and APC: the Yin and Yang of cell cycle regulated proteolysis. *Curr. Opin. Cell Biol.* 10:759–768.

Pfleger, C.M., and M.W. Kirschner. 2000. The KEN box: an APC recognition signal distinct from the D box targeted by Cdh1. *Genes Dev.* 14:655–665.

Prokopenko, S.N., A. Brumby, L. O'Keefe, L. Prior, Y. He, R. Saint, and H.J. Bellen. 1999. A putative exchange factor for Rho1 GTPase is required for initiation of cytokinesis in *Drosophila*. *Genes Dev.* 13:2301–2314.

Prokopenko, S.N., R. Saint, and H.J. Bellen. 2000. Untying the Gordian knot of cytokinesis. Role of small G proteins and their regulators. *J. Cell Biol.* 148: 843–848.

Rappaport, R. 1997. Cleavage furrow establishment by the moving mitotic apparatus. *Dev. Growth Differ.* 39:221–226.

Ridley, A.J., A.J. Self, F. Kasmi, H.F. Paterson, A. Hall, C.J. Marshall, and C. Ellis. 1993. rho family GTPase activating proteins p190, bcr and rhoGAP show distinct specificities in vitro and in vivo. *EMBO J.* 12:5151–5160.

Roof, R.W., M.D. Haskell, B.D. Dukes, N. Sherman, M. Kinter, and S.J. Parsons. 1998. Phosphotyrosine (p-Tyr)-dependent and -independent mechanisms of p190 RhoGAP-p120 RasGAP interaction: Tyr 1105 of p190, a substrate for c-Src, is the sole p-Tyr mediator of complex formation. *Mol. Cell. Biol.* 18: 7052–7063.

Settleman, J., V. Narasimhan, L.C. Foster, and R.A. Weinberg. 1992. Molecular cloning of cDNAs encoding the GAP-associated protein p190: implications for a signaling pathway from ras to the nucleus. *Cell.* 69:539–549.

Somers, W.G., and R. Saint. 2003. A RhoGEF and Rho family GTPase-activating protein complex links the contractile ring to cortical microtubules at the onset of cytokinesis. *Dev. Cell.* 4:29–39.

Sordella, R., M. Classon, K.Q. Hu, S.F. Matheson, M.R. Brouns, B. Fine, L. Zhang, H. Takami, Y. Yamada, and J. Settleman. 2002. Modulation of CREB activity by the Rho GTPase regulates cell and organism size during mouse embryonic development. *Dev. Cell.* 2:553–565.

Sordella, R., W. Jiang, G.C. Chen, M. Curto, and J. Settleman. 2003. Modulation of Rho GTPase signaling regulates a switch between adipogenesis and myogenesis. *Cell.* 113:147–158.

Straight, A.F., and C.M. Field. 2000. Microtubules, membranes and cytokinesis. *Curr. Biol.* 10:R760–R770.

Tatsis, N., D.A. Lannigan, and I.G. Macara. 1998. The function of the p190 Rho GTPase-activating protein is controlled by its N-terminal GTP binding domain. *J. Biol. Chem.* 273:34631–34638.

Tikoo, A., S. Czekay, C. Viars, S. White, J.K. Heath, K. Arden, and H. Maruta. 2000. p190-A, a human tumor suppressor gene, maps to the chromosomal region 19q13.3 that is reportedly deleted in some gliomas. *Gene.* 257:23–31.

Tominaga, T., E. Sahai, P. Chardin, F. McCormick, S.A. Courtneidge, and A.S. Alberts. 2000. Diaphanous-related formins bridge Rho GTPase and Src tyrosine kinase signaling. *Mol. Cell.* 5:13–25.

Wang, D.Z., M.S. Nur-E-Kamal, A. Tikoo, W. Montague, and H. Maruta. 1997. The GTPase and Rho GAP domains of p190, a tumor suppressor protein that binds the M(r) 120,000 Ras GAP, independently function as anti-Ras tumor suppressors. *Cancer Res.* 57:2478–2484.

Wang, Z., P.S. Tung, and M.F. Moran. 1996. Association of p120 ras GAP with endocytic components and colocalization with epidermal growth factor (EGF) receptor in response to EGF stimulation. *Cell Growth Differ.* 7:123–133.

Wolf, R.M., N. Draghi, X. Liang, C. Dai, L. Uhrbom, C. Eklof, B. Westermark, E.C. Holland, and M.D. Resh. 2003. p190RhoGAP can act to inhibit PDGF-induced gliomas in mice: a putative tumor suppressor encoded on human Chromosome 19q13.3. *Genes Dev.* 17:476–487.

Yoshizaki, H., Y. Ohba, K. Kurokawa, R.E. Itoh, T. Nakamura, N. Mochizuki, K. Nagashima, and M. Matsuda. 2003. Activity of Rho-family GTPases during cell division as visualized with FRET-based probes. *J. Cell Biol.* 162:223–232.

Zeitlin, S.G., and K.F. Sullivan. 2001. Animal cytokinesis: breaking up is hard to do. *Curr. Biol.* 11:R514–R516.